Environmental heterogeneity drives tsetse fly population dynamics

Hélène Cecilia[1], Sandie Arnoux[1], Sébastien Picault[1,2], Ahmadou Dicko[3,4], Momar Talla Seck[5], Baba Sall[6], Mireille Bassène[5], Marc Vreysen[7], Soumaïla Pagabeleguem[8,9], Augustin Bancé[10], Jérémy Bouyer[3,4,7,11], Pauline Ezanno[1*]

[1]*BIOEPAR, INRA, Oniris, CS40703, 44307 Nantes, France*
[2]*Univ. Lille, CNRS, Centrale Lille, UMR9189 CRIStAL, Lille, France*
[3]*Unité Mixte de Recherche ASTRE 'Animal, Santé, Territoires, Risques et Ecosystèmes', Campus international de Baillarguet, Centre de Coopération Internationale en Recherche Agronomique pour le Développement (CIRAD), 34398 Montpellier, France*
[4]*ASTRE, University of Montpellier, CIRAD, INRA, Montpellier, France*
[5]*Institut Sénégalais de Recherches Agricoles, Laboratoire National d'Elevage et de Recherches Vétérinaires, Dakar-Hann, Sénégal*
[6]*Direction des Services vétérinaires, Ministère de l'Elevage et des Productions animales, Sphères ministérielles de Diamniadio, Bât. C, 3ème étage, Sénégal*
[7]*Insect Pest Control Laboratory, Joint FAO/IAEA Programme of Nuclear Techniques in Food and Agriculture, 1400 Vienna, Austria*
[8]*Insectarium de Bobo-Dioulasso – Campagne d'Eradication des Tsé-tsé et Trypanosomoses (IBD-CETT), Bobo-Dioulasso 01 BP 1087, Burkina Faso.*
[9]*Université de Dédougou (UDDG), BP 176, Burkina Faso.*
[10]*Centre International de Recherche-Développement sur l'Elevage en Zone Subhumide (CIRDES), Bobo-Dioulasso 01 01 BP. 454, Burkina Faso.*
[11]*Unité Mixte de Recherche `Interactions hôtes-vecteurs-parasites-environnement dans les maladies tropicales négligées dues aux trypanosomatides', CIRAD, Montpellier, France*

[*]*Corresponding author's Email: pauline.ezanno@inra.fr*

Keywords: Disease vectors | Mechanistic modelling | Spatio-temporal dynamics | Experimental and field data | Mortality scenarios

Abstract

A spatially and temporally heterogeneous environment may lead to unexpected population dynamics, and knowledge still is needed on which of the local environment properties favour population maintenance at larger scale. As regards pathogen vectors, such as tsetse flies transmitting human and animal African trypanosomosis, such a knowledge is crucial for proposing relevant management strategy. We developed an original mechanistic spatio-temporal model of tsetse fly population dynamics, accounting for combined effects of spatial complexity, density-dependence, and temperature on the age-structured population, and parametrized with field and laboratory data. We confirmed the strong impact of temperature and adult mortality on tsetse populations. We showed that patches with the lowest mean temperatures and lowest variations act as refuges when adult mortality is homogeneously increased. Our results highlighted the importance of baseline data collection to characterize the targeted ecosystem before any control measure is implemented to maximize its efficiency.

1. Introduction

Environmental spatial heterogeneity is a key driver of population dynamics (Tilman & Kareiva 1997; Vinatier et al. 2011), inducing movements from source to sink patches possibly enhancing population persistence in unsuitable patches (Holt 1985; Pulliam 1988). In addition, environmental suitability varies over time both at local scale, due to microclimate variations as related to vegetation growth (Keppel et al. 2017), and at large scale, due to a seasonal occurrence of unfavourable periods. Confounding the role of spatial and temporal environmental heterogeneity potentially gives rise to erroneous predictions of ecological processes (Clark 2005). However, relating such a complex time- and space-varying habitat with population dynamics still is a challenge in ecology (Sutherland et al. 2013; Crone 2016; Griffith et al. 2016). Therefore, illustrative examples about the complex interplay between spatio-temporal environmental variability and population dynamics are welcome to feed theory and assess which patch properties (co)contribute to define sources and sinks in heterogeneous environments.

This is particularly true when it comes to controlling infectious diseases, given that vector-borne disease dynamics is largely determined by those of vector populations (Hartemink et al. 2015). First, spatial heterogeneity is expected to favour vector persistence thanks to the rescue effect, especially if control is not area-wide, i.e. targeting an entire insect pest population within a circumscribed area (Reichard 2002; Hendrichs et al. 2007). Second, such populations and associated pathogens face seasonal variations of habitat suitability (Charron et al. 2013). Environmental suitability varying in space and time could induce unexpected population dynamics, potentially impairing its management, whereas control strategies are nonetheless often elaborated without considering local environmental specificities.

Tsetse flies (*Glossina* spp.) are vectors of African trypanosomes, widely recognized as a major pathological constraint for efficient livestock species and agricultural development in sub-Saharan Africa (Alsan 2015). *Trypanosoma* spp. parasites both cause Human African Trypanosomosis and African Animal Trypanosomosis. Widely distributed, they occur in 38 countries and infest 10 million

27 km^2 (Vreysen et al. 2013), with over 60 million people continuously exposed to the risk of infection
28 of this neurological, potentially lethal disease, mainly in remote rural areas with limited access to
29 health services. Besides, farms in tsetse-infested areas suffer a 20% to 40% loss in livestock
30 productivity, adding up to an estimated $4500 million loss annually for producers and consumers in
31 sub-Saharan Africa (Budd 1999). Among the 31 species and subspecies known of tsetse flies, a third
32 is of economic (agricultural and veterinary) and sanitary importance (Solano et al. 2010a). Efforts to
33 manage the vector and the disease in Africa are on-going for decades but largely fail to create
34 sustainable tsetse free areas, resulting in only a reduction of less than 2% of tsetse distribution
35 (Allsopp 2001; Bouyer et al. 2013a). Although tsetse flies turned out to be extremely complex species,
36 their very low rate of reproduction would make them a relevant target to eradicate, making crucial to
37 better apprehend their spatio-temporal population dynamics (Peck & Bouyer 2012).
38 Mathematical models have proved to be relevant tools in ecology, to better understand the dynamics
39 of populations (Hasting 2012) and to predict such dynamics under modified conditions (Evans et al.
40 2012). Process-based models incorporate at minimal costs sparse and heterogeneous knowledge from
41 various areas, species, and fields of expertise. Simulations are complementary to field observations
42 and experiments (Restif et al. 2012), enabling the fast acquisition of quantitative predictions which
43 can in turn emphasize the need for further biological investigations. Moreover, the range of
44 behaviours of complex systems can be scanned using mechanistic models, and scenarios are tested
45 easily (Cailly et al. 2012). Provided hypotheses and limits are clearly stated (Getz et al. 2018), models
46 can guide decision-making (Sutherland & Freckleton 2012).
47 As regards tsetse biology and population dynamics, entomologists quickly realized how useful
48 models could be (Rogers 1988, 1990; and more recently: Vale & Torr 2005; Lin et al. 2015), and
49 encouraged their use when designing management decisions (Hargrove 2003; Childs 2011; Meyer et
50 al. 2018). However, most models have failed to predict the persistence of target populations leading
51 to misleading guidelines for control programs (Peck & Bouyer 2012; Bouyer et al. 2013b). Most of
52 these programs were not implemented following area-wide principles (Klassen 2005) and their failure

could be imputed to population resurgence in non-eradicated patches or re-invasion of the targeted zone by neighbouring populations (Meyer et al. 2016; Lord et al. 2017). However, it is still unclear what the relevant patch properties are and how they combine to define sources and sinks in a hostile environment created by eradication efforts. To address such an issue, the spatial complexity of the environment has to be accounted for. While omitted in most models until recently, it has been shown to considerably influence predictions once incorporated (Peck 2012; Barclay & Vreysen 2013; Lord et al. 2017). Indeed, population dynamics is expected to vary locally among patches of variable suitability, possibly affecting population dynamics at large metapopulation scale. To better assess how large scale tsetse fly population dynamics are affected by local dynamics, there is a need for an integrated spatio-temporal model thoroughly evaluated against field and experimental data, and fed by environmental data to account for landscape heterogeneity.

To assess if spatial and temporal environmental heterogeneity drives tsetse fly population dynamics at large scale, we developed an original mechanistic spatio-temporal model of tsetse fly population dynamics and incorporated environmental heterogeneity through a data-driven approach. The model was applied to *Glossina palpalis gambiensis* in the Niayes (Senegal), a region with an ongoing eradication project (Dicko et al. 2014). In this area, less than 4% of the habitat is suitable (Bouyer et al. 2010), and tsetse flies harbour a metapopulation structure (Solano et al. 2010b). This knowledge was incorporated in the model, accounting for combined effects of spatial complexity, density-dependence, and temperature on the age-structured population.

2. Material and methods

Key knowledge on tsetse biology

Meteorological variables influence the abundance and spatial distribution of arthropod disease vectors (Hay et al. 1996). For tsetse flies, effect magnitude depends on species (Rogers & Randolph 1991; Rogers et al. 1996; Hargrove 2001), but average temperature is the most influent

77 meteorological variable on life cycle (Hargrove 2004). However, its influence compared to or
78 combined with demographic processes is barely known.
79 The tsetse fly is adenotrophic viviparous: the egg hatches in the female and the larva is nourished by
80 dedicated organs until larviposition. A temperature decrease lengthens the time between
81 larvipositions (Harley 1968). Similarly, the colder it gets in breeding sites, the longer the pupa
82 development (Glasgow 1963; Phelps & Burrows 1969a,b). After pupa emergence, the newly emerged
83 fly (teneral) takes its first blood meal to strengthen its musculature and reproduce. The first oocyte
84 maturation into pupa takes around 18 days, making the first larviposition longer than subsequent ones
85 (10 days) depending on species and temperature (Hargrove 2004).
86 Extreme temperatures, cold or warm, increase fly mortality (Hargrove 2001). Mortality, related to
87 predation and feeding success, is density-dependent (Rogers & Randolph 1984) and age-dependent
88 (Hargrove 1990), with remarkably high losses in tenerals partly due to starvation risk (Phelps &
89 Clarke 1974; Hargrove 2004). Learning capacities of older flies make them return on their first host,
90 increasing their hunting efficiency with age (Bouyer et al. 2007).
91 Tsetse flies are classified into three groups of different behaviours and distributions: forest (subgenus
92 *Fusca*), savannah (subgenus *Morsitans*), and riverine flies (subgenus *Palpalis*). Most of previous
93 model concerned *Glossina pallidipes* and *G. morsitans*, both of the savannah group. We focused on
94 *G. p. gambiensis*, a riverine fly living in forest galleries and riparian thickets (Bouyer et al. 2005).
95 Due to habitat characteristics, this species is known to mostly disperse in one dimension (along
96 rivers). However, climate changes induce the disappearance of rivers and associated vegetation as
97 evidenced in our study area (Niayes, Senegal, Fig. 1). *G. p. gambiensis* adapted to patchy vegetation
98 mainly associated to human watering activities (Bouyer et al. 2010), dispersing in two dimensions.
99 Furthermore, isolated populations in fragmented habitats are preferential targets for area-wide
100 integrated pest management programs (Hendrichs et al. 2007; Bouyer et al. 2015). Hence, our case
101 study is of broad relevance for better understanding and predicting tsetse fly spatio-temporal

population dynamics in rapidly changing ecosystems that are gradually becoming the norm (Guerrini et al. 2008).

Data on tsetse biology

Variations in mortality and fecundity with temperature were measured for the studied strain under experimental conditions (Pagabeleguem et al. 2016). We used data on the first larval period (time between emergence and first pupa production) and on subsequent inter-larval periods (time between reproductive cycles). As the colony was maintained at 24°C with only temperatures above 24°C tested to assess the maximum critical temperature for flies, most data used to estimate female mortality were obtained at 24°C and none at a lower temperature. In addition, the effect of temperature on *G. p. gambiensis* pupal duration was measured under experimental conditions (Centre International de Recherche-Développement sur l'Elevage en zones Subhumides, CIRDES, Bobo-Dioulasso, Burkina Faso, 2009). One hundred and twenty 20-day old pupae were hold in climate controlled rooms until emergence. The experiment was replicated three times for each temperature tested (Table S1).

Dispersing abilities of *G. p. gambiensis* were assessed from release-recapture data of marked sterile males (Oct. 2010 to Dec. 2012; Pagabeleguem 2012). Flies were mass-reared in CIRDES Burkina Faso and shipped as irradiated pupae to Senegal (Pagabeleguem et al. 2015). Flies were released twice a month in four locations (Parc de Hann in Dakar, Diacksaw Peul, Pout, and Kayar; Fig. 1). Two release points were selected per location (in suitable vs. unsuitable habitats). Released flies were trapped using Vavoua traps (Laveissière & Grébaut 1990) up to 2kms from release points. Distance between traps varied between 100m and 300m. Traps were set in the morning before 9:00 and collected in the afternoon after 16:00, every 3 days. The monitoring of a release stopped when less than 2 marked males were recaptured.

In another study, natural abortion rate was monitored in Hann, Diacksaw, Sebikotane, and Pout (Fig. 1). Ten traps per site were deployed monthly from March 2008 to February 2009, and then every three months until September 2010 (Hann, Diacksaw) or December 2011 (Pout, Sebikotane). Flies were collected at least once a day. Fresh flies were dissected to estimate their ovarian sequence. This

female dataset was used to calculate the population age structure, to be compared to simulation results for partial validation.

Environmental data

The spatio-temporal heterogeneity of the environment was realistically represented using an original data-driven approach. The environmental carrying capacity and the local daily temperatures were incorporated in the model.

The carrying capacity was defined as the maximum sustainable number of individuals for a given area and was estimated as (Eq. 1):

$$k = \frac{SI \times ADT}{\sigma} \quad \text{(Eq. 1)}$$

with *SI* the suitability index, estimated with a species distribution model (Dicko et al. 2014) based on the maximum entropy (Maxent) (Supporting Information 2.1), σ the trap efficiency, i.e. the probability that a trap catches a fly within 1km² within a day (Barclay and Hargrove 2005), and *ADT* the apparent density of flies per trap per day (Dicko et al. 2015). All available data from catches obtained between 2007 and 2010 in the Niayes before the start of the eradication campaign were used to estimate local carrying capacities (Supporting Information 2.1).

Air temperatures measured in weather stations are not those experienced by flies in resting places. Indeed, flies prefer microenvironments that are 2-6°C lower than the ambient temperature (Hargrove & Coates 1990). In addition, temperature largely varies from the centre of a gallery forest towards its edges (Bouyer 2006). Therefore, micro-climate and approximated local temperatures truly perceived by tsetse flies were explicitly modelled using input data from weather stations transformed using a spatio-temporal geostatistical model (Kilibarda et al. 2014). Available temperature data recorded in selected suitable patches were used to correct the bias present in moderate resolution imaging spectroradiometer (MODIS) Land-Surface Temperature (macro-climate; Supporting Information 2.2). High resolution macro-climate data were available only for 2011. Approximated temperatures

were used as model inputs in a zone known as suitable for tsetse to check if the simulated population persisted as expected.

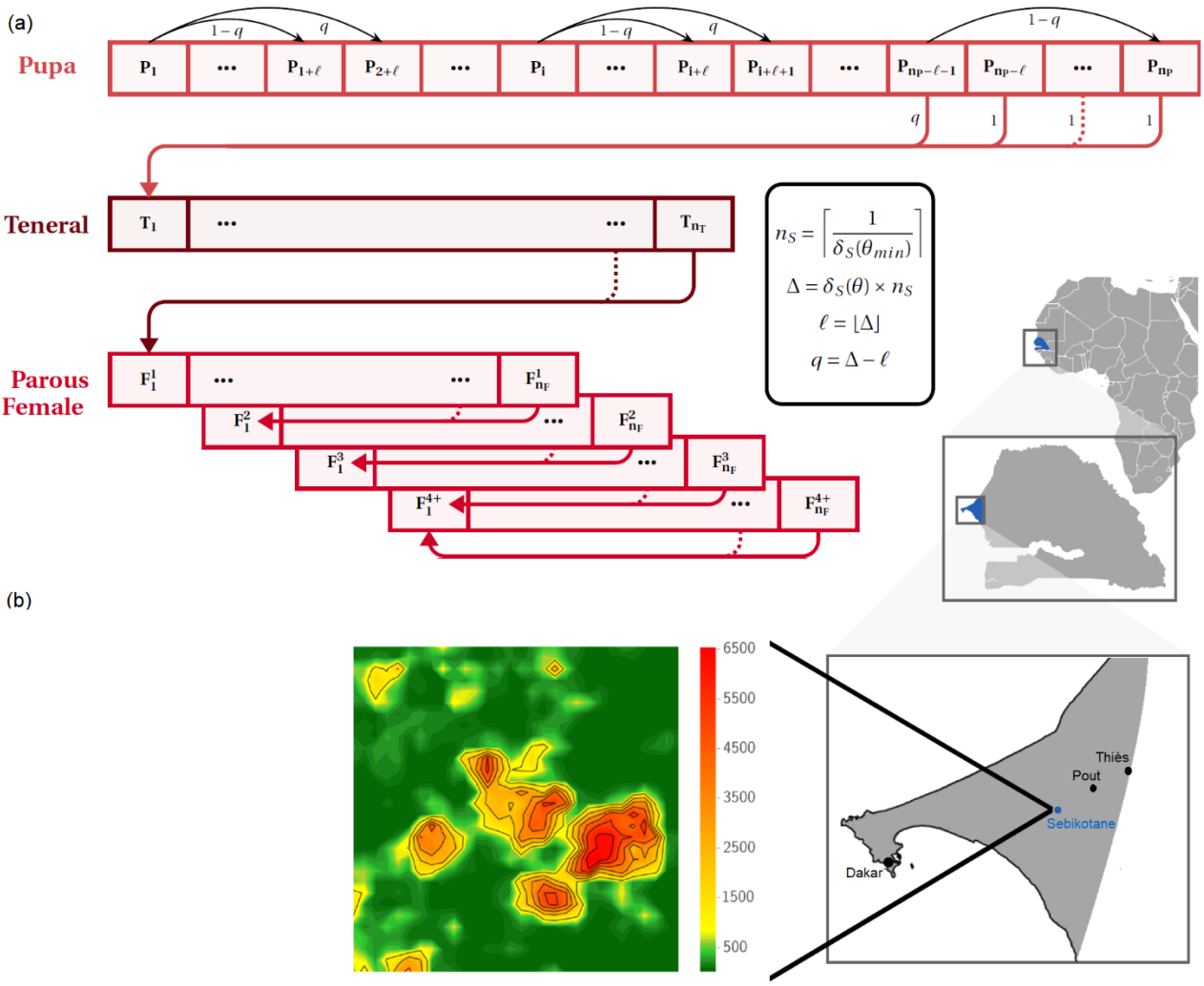

Figure 1. Local and general tsetse fly population dynamics applied to the Niayes in Senegal. (a) within-cell model diagram of tsetse fly populations dynamics (time unit is a day). All transitions between stages except P to T triggers the birth of a new pupa P_1. Transitions occur at a development rate δ_S for stage S according to temperature $\theta_{t,c}$ at time t in cell c, giving rise daily to a minimum jump of l states from each state i of stage S, with $(1\text{-}q)S_{t,c,i}$ individuals going from state $S_{t,c,i}$ to state $S_{t+1,c,i+l}$ and $pS_{t+1,c,i}$ individuals going to $S_{t+1,c,i+l+1}$. If $i + l > n_S$ (respectively $i + l + 1 > n_S$), then concerned individuals go to the next stage. Stage $S \in \{P, T, F_x, M\}$, parity $x \in \{1, 2, 3, 4+\}$. (b) Map of Senegal identifying areas providing field data and localizing the 30x30 simulated area, highlighting the spatial heterogeneity in local carrying capacities k_c (inbox, scale in number of individuals).

A mechanistic spatio-temporal model of tsetse fly population dynamics

A mechanistic and deterministic compartmental model was developed to predict the spatio-temporal tsetse fly population dynamics accounting for environmental heterogeneity and including density-dependence. Individuals were categorized into pupae (P), without differentiating males and females,

158 tenerals (T, immature nulliparous females), and parous females with four stages (F_1, F_2, F_3, F_{4+}; Fig.
159 1a) in agreement with ovarian dissection which provides accurate information about the first four
160 parities (Hargrove & Ackley 2015). Adult males (M) were not considered limiting for breeding. They
161 could mate from the age of 6 days, regardless of temperature, after which they were only subject to
162 mortality. They played a role in density-dependent processes. The environment was modelled using
163 a grid (cell resolution: 250m x 250m; study area: 30 x 30 cells; Fig. 1b). The model was developed
164 in Python as a discrete-time model with a one-day time step (Supporting Information 6).
165
166 ***Within-cell dynamics*** **-** The population size of life stage *S* at time *t* in cell *c* decreased with mortality,
167 following a negative exponential model of instantaneous rate $\mu_{S,t,c}$ (Eq. 2). Considering the lack of
168 data on pupa mortality, we used a constant rate (Eq. 3) of 0.01 day^{-1} (Childs 2011). For adults, the
169 log of mortality rates increased linearly with temperature after 24°C (Hargrove 2004). Below this
170 threshold, and for the range of temperatures observed in the field, the literature and the lack of data
171 suggested a constant mortality rate (Eq. 4). Age-dependence was featured by setting teneral mortality
172 to twice that of mature females (Eq. 5). Density-dependence occurred when the adult population
173 exceeded the cell carrying capacity (Eq. 6-7, Hargrove 2004).

174 $S_{t+\Delta t,c} = S_{t,c}e^{-\mu_{S,t,c}\Delta t}$, with stage $S \in \{P, T, F_x, M\}$, parity $x \in \{1, 2, 3, 4+\}$, $\Delta t = 1$ (Eq. 2)

175 $\mu_P = m_P$ (Eq. 3)

176 $$\mu_{X,t,c} = \begin{cases} \mu_{X,t,c}(\theta_{t,c} = 24°C), if\, \theta_{t,c} \leq 24°C \\ \mu_{X,t,c}(\theta_{t,c}), if\, \theta_{t,c} > 24°C \end{cases}, X \in \{T, F, M\}$$ (Eq. 4)

177 $\mu_{T,t,c} = 2\mu_{F,t,c}$ (Eq. 5)

178 $\mu_{X,t,c} = \beta_{t,c}e^{m_{1,X}\theta_{t,c}+m_{2,X}}$, $X \in \{F, M\}$ (Eq. 6)

179 $$\beta_{t,c} = \begin{cases} 1, if\, \frac{A_{t,c}}{k_c} \leq 1 \\ \frac{A_{t,c}}{k_c}, if\, \frac{A_{t,c}}{k_c} > 1 \end{cases}, \text{with } A_{t,c} = T_{t,c} + \sum_{i=1}^{4} F_{i,t,c} + M_{t,c}$$ (Eq. 7)

In addition, individuals evolved within and between stages as a function of temperature. Pupa development function $\delta_{P,t,c}$ was fitted on data. For adults and tenerals, consistency of experimental data on the target species was checked against published equations (Hargrove 2004; Eq. 8; Fig. 2):

$$\delta_{X,t,c} = d_{1,X}(\theta_{t,c} - 24) + d_{2,X}, X \in \{T, F\} \quad \text{(Eq. 8)}$$

Each stage was discretized into n_S states, n_S being the longest duration in stage S obtained with its development rate δ_S calculated at the minimum temperature of the year $min(\theta_{t,c})$ (Fig. 1a). For higher temperatures, individuals made a leap forward in the development vector, the interval being determined by the integer part l of Δ (Eq. 9, Fig. 1a).

$$\Delta_{S,t,c} = \delta_{S,t,c}(\theta_{t,c})n_S \quad \text{(Eq. 9)}$$

To avoid discretization artefacts, individuals were proportionally divided into two successive states according to the decimal part q of Δ (Fig. 1a). Individuals who reached state n_S evolved to the next stage, a pupa being produced if teneral or adult females were concerned. After the fourth parity, females looped back to the start of F_{4+}.

Between-cell dynamics - An original dispersal pattern was designed favouring suitable over hostile habitats to align with species behaviour. The proportion $p_{t,c}$ of flies leaving cell c at time t was controlled by a sigmoidal density-dependent dispersal rate (Lloyds-Smith, 2010), adapted for individuals competing to access resources (Rogers & Randolph 1984) (Eq. 10):

$$p_{t,c} = \frac{1}{1+e^{-g\left(\frac{A_{t,c}}{k_c}-1\right)}} \quad \text{(Eq. 10)}$$

with k_c the carrying capacity in cell c, $A_{t,c}$ the number of adults in cell c at time t, and g a shape parameter set to 10 meaning that $p_{t,c}\begin{cases}\approx 0, if A_{t,c} < 0.5k_c \\ \approx 1, if A_{t,c} > 1.5k_c \\ 0.5, if A_{t,c} = k_c\end{cases}$ (Fig. S1).

The spatial distribution of dispersing flies from cell c to neighbouring cells $Prob_{c\to i\in\{v\}}$ was set by the relative attractiveness of neighbouring cells $a_{t,i\in\{v\}}$ (Eq. 11-12). This attractiveness was designed to favour the emptiest cells ($A_{t,i} \ll k_i$) and cells of greatest k_i if equal $A_{t,i}$. An extended Moore

neighbourhood of range r was used: flies dispersed from a cell to its $(2r + 1)^2$ neighbours (v), including the cell itself and diagonals. Parameter r is the maximum distance reached daily, in number of cells, rather than the effective distance covered per fly per day, as the trajectory is not linear. It was calibrated on data by looking at the average $\frac{distance(m)}{time(days)}$ between release and capture of marked flies (Fig. S2).

$$a_{t,i\in\{v\}} = \frac{\left(1-e^{\frac{-k_i}{A_{t,i}}}\right)k_i}{max\left(k_{i\in\{v\}}\right)} \quad \text{(Eq. 11)}$$

$$Prob_{c\to i\in\{v\}} = \frac{a_i}{\sum_{j\in v} a_j} \quad \text{(Eq. 12)}$$

Model analysis

The reference scenario was examined (parameter values provided in Table S2). The individual and joint effects of input variations on aggregated output variance (Table S3) were evaluated through a global sensitivity analysis. Population size and age structure were outputs of interest. As traps do not capture tenerals and old females as efficiently as females of intermediate parities (Sanders 1962), predicted age structure was compared with field data for $\frac{F_{i=1,2,3}}{F_1+F_2+F_3}$.

A 3-year burn-in period was simulated starting with $T_{0,c}=M_{0,c}=0.5k_c$ ($A_{0,c}=k_c$), using reference parameter values. Then, parameter values of each of the tested scenarios were applied for three more years. Carrying capacities were spatially heterogeneous (Fig. 1b) but assumed constant over time. Perceived temperatures, estimated daily per cell for a year, were repeated between years.

A variance-based global sensitivity analysis was performed using the Fourier Amplitude Sensitivity Testing (FAST) method (Saltelli et al. 2008). Mortality and development functions of each life stage were tuned with weighting coefficients. A common weight was applied to all adult mortalities (T, M, $F_{1:4+}$) to preserve model hypotheses. A weighting coefficient also was applied to carrying capacities, thus regulating density-dependence magnitude. As the dispersal rate should remain in the range [0-1], the shape parameter g was varied (Fig. S1). Parameters varied by ± 5% of their reference value.

The same range, when applied to temperature, changed the annual mean by more than 2°C, which was far greater than what was observed. Therefore, a variation of ±0.3°C was used, corresponding to the average deviation from the daily mean in the area (Fig. S4). First order and interaction sensitivity indices were calculated per parameter (Saltelli et al. 2008).

Evaluation of control strategies

A control strategy was mimicked by increasing adult mortality (from +2.5% to +100%) homogeneously in space, and assessed with respect to the female population ($T+F_{1:4+}$) over time (every year for 5 years) and space. At the end of simulations, two ratios were computed : $\frac{T_{t_{max},c}+F_{1:4+,t_{max},c}}{\sum_c T_{t_{max},c}+F_{1:4+,t_{max},c}}$ highlighted cells contributing the most to the female population in the area, while $\frac{(T_{t_{max},c}+F_{1:4+,t_{max},c})_{scenario}}{(T_{t_{max},c}+F_{1:4+,t_{max},c})_{reference}}$ quantified the local impact of increased mortality compared to natural levels. The correlation between environmental variables and the spatial structure of the remaining population was assessed.

3. Results

New insights from biological data

New equations were calibrated for temperature-dependent processes of the life cycle of tsetse flies combining published and new observed data (Fig. 2). The log-linear function for adult mortality (Table S2) differed from published ones for other species (Fig. 2a). Up to 24°C, female mortality rate was 0.013 day^{-1}, then it grew exponentially to reach 0.023 day^{-1} at 32°C. Male mortality was higher than female one (Table S2, Fig. S3).

Pupa emergence clearly followed a logistic equation when fitted on observed data, providing a new pattern compared to Hargrove's equation (2004) (Fig 2b, Eq. 15, Table S4).

$$\delta_{P,t,c} = \left(d_{1,P} + \frac{d_{2,P} - d_{1,P}}{1 + e^{\frac{d_{3,P} - \theta_{t,c}}{d_{4,P}}}} \right)^{-1} \quad \text{(Eq. 15)}$$

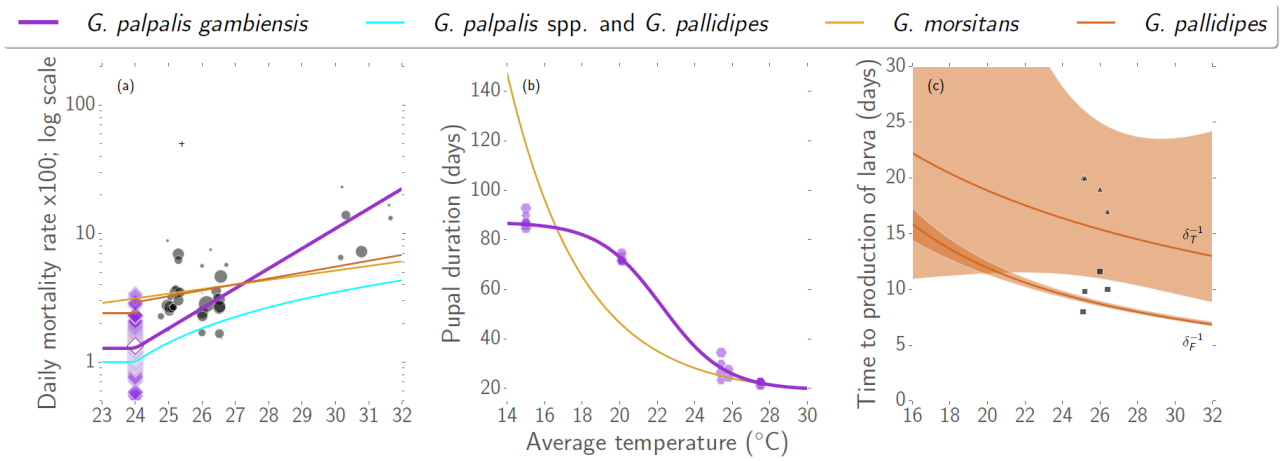

Figure 2. Data (as dots) and predictions (as lines) fitted on new data (if relevant) and from literature for temperature-dependent processes of the model: (a) adult female daily mortality rate (in log-scale); (b) pupal duration (in days); (c) time to larviposition for tenerals (T, upper curve, triangles) and parous females (F, lower curve, squares). Data from Pagabeleguem et al. (2016) is shown in grey (the cross in (a) was considered an outlier). New data on *G. p. gambiensis* (from FAO/IPCL and CIRDES) is shown in purple, with the barycentre of mortality rate at 24°C highlighted as a white-filled diamond. Purple thick lines are the newly calibrated equations used in the population dynamics model. Predictions from Barclay's equation (2011) is in cyan. Orange lines correspond to predictions from Hargrove's equations (2004), with filled areas in (c) corresponding to prediction intervals. Equations for time to larviposition were not modified as only few new data was available, which is consistent with Hargrove's equation.

Mark-release-recapture data indicated a dispersal range *r* of one cell, the daily average distance proved to be less than 250m (Fig. S2).

Finally, the spatial heterogeneity of carrying capacities was high, ranging from 7 to 6548 individuals (median: 145) per cell. On the contrary, spatial variations of local temperatures were small, the standard deviation over the grid never exceeding 0.67°C at any time step.

Reference scenario analysis

The reference scenario was closely in line with field observations made before the start of the Niayes' control program (Fig. 3). Population dynamics was seasonal (Fig. 3b), and driven by temperature as expected (Fig. 3a). Female population ($T+F_{1:4+}$) was stable across years with a growth rate of -0.75% the last simulation year. As observed (Fig. 3d), females between first and third larviposition ($F_1+F_2+F_3$) were distributed on average for 40% in F_1, 33% in F_2, and the rest in F_3 (Fig. 3c). The spatial variability of age structure was 3 to 4 times lower than its temporal variability.

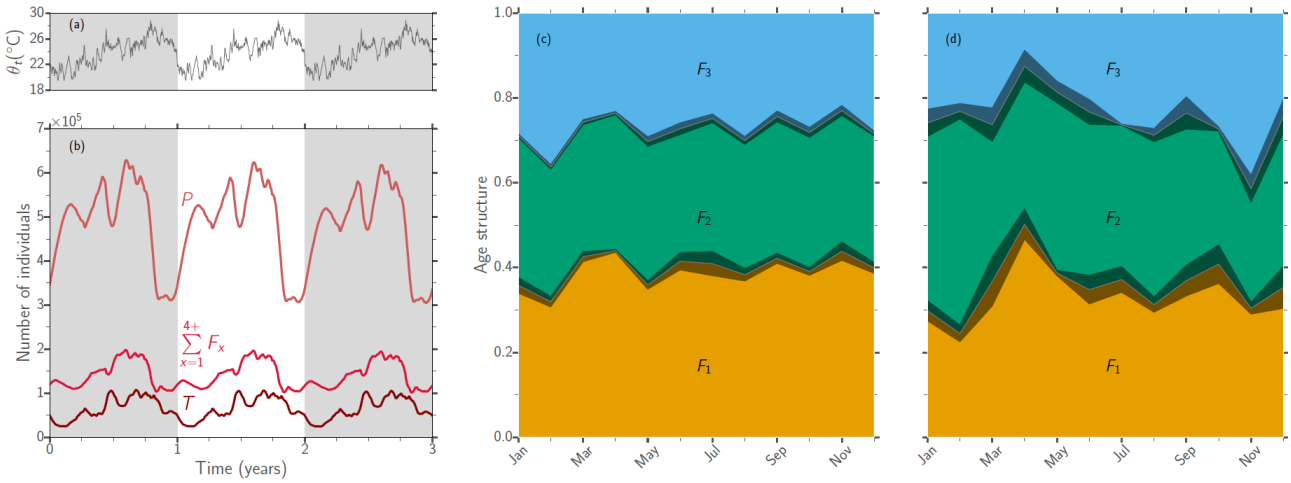

Figure 3. Model predictions for the reference scenario: (a) average daily temperatures over three years (in °C); (b) total number of individuals per stage (P: pupae, T: tenerals, F: parous females) in the grid (56.25 km^2) over three years of simulation; (c) female age structure ($\frac{F_{i=1,2,3}}{F_1+F_2+F_3}$) during the last year of simulation; (d) observed female age structure (captures and dissection occurred from 2008 to 2011 in the Niayes; results were averaged by month, all years and locations aggregated; grey filled areas are confidence intervals around the mean: $\frac{\pm 1.96 \times sd_{month}}{\sqrt{n_{month}}}$, with sd_{month} the standard deviation and n_{month} the number of measures, i.e. the number of days in the month for simulations, the number of captures for data).

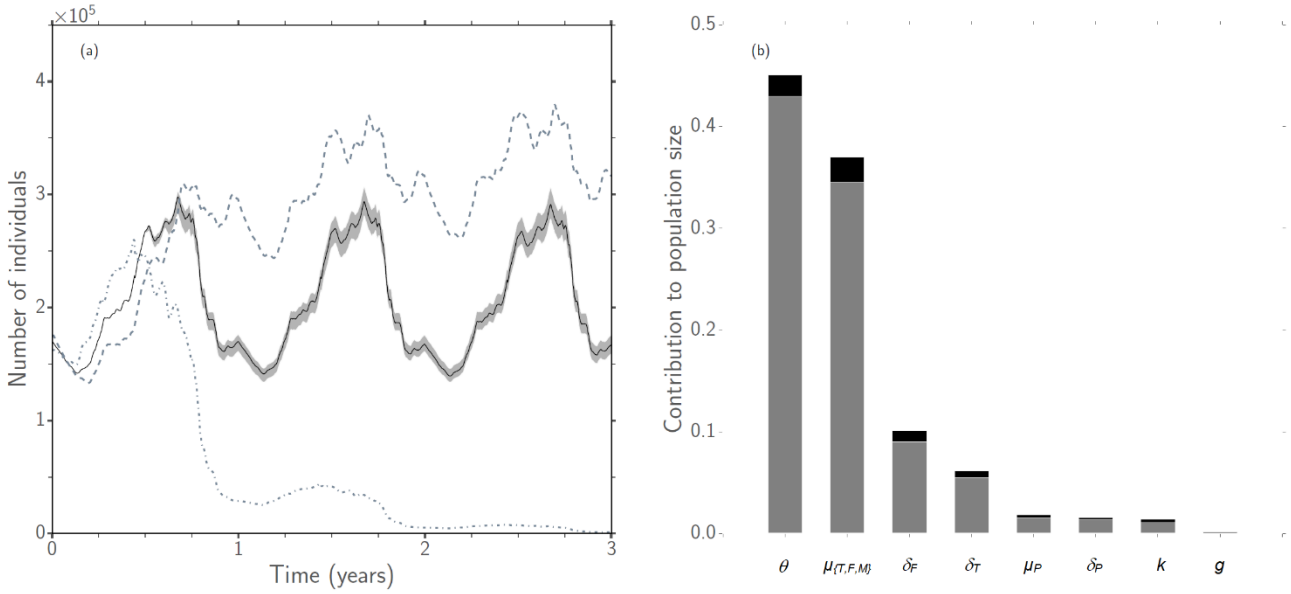

Figure 4. Sensitivity analysis of the model: (a) effect on population size (teneral and adult females) of temperature variations (+5% from reference: dash dot, -5%: dashed) compared to ±5% variations in carrying capacities (grey filling); (b) results of the FAST sensitivity analysis with contribution to population size variance of model parameters (θ: temperature, $\mu_{\{T,F,M\}}$: adult mortality, δ_X: development of stage X (with X in {F: adult females, T: tenerals, P: pupae}), k: carrying capacities, g: the shape parameter in the diffusion process; sensitivity indices for principal effect in grey and for first order interactions in black). All parameters were varied by ±5% from their reference value except temperature varying by ±0.3°C.

Temperature and mortality as key factors driving population size

Model predictions other than age structure (Fig. S5) were highly sensitive to temperature (T) and adult mortality ($\mu_{\{T,F,M\}}$) variations, and moderately to teneral (δ_T) and parous (δ_F) female development variations (Table S4), while parameters related to pupae (μ_P, δ_P), carrying capacities (k), and dispersal (g) did not contribute to output variance (Fig. 4, Fig. S6). A 5% variation in temperature lead to demographic explosion or extinction, substantially outweighing the effect of a similar variation in carrying capacities (Fig. 4a), reinforcing the need for considering reasonable temperature variations. Temperature and adult mortality explained 78% of population size variance (Fig. 4b). Development of tenerals and parous females added up to another 14.5% of explained variance. Unexpectedly, interactions between parameters were not important.

Efficiency of control measures driven by environmental heterogeneity

Increasing adult mortality at levels comparable to what can be obtained during control programs (Hargrove 2003) induced a quick population decline (Fig. 5). A 50% augmentation (i.e. a parous female daily mortality rate of 2.94 day^{-1} and a life expectancy of 51.5 days at 24°C) resulted in a 90% decrease in the female population ($T+F_{1:4+}$) in one year (Fig. 5a).

Once reaching low local densities, new patterns emerged related to cell-specific properties. On the one hand, as expected, the spatial distribution of individuals was clearly linked to carrying capacities (Fig. 1 vs. Fig. 5b1-3). The greater the adult mortality, the more uneven was the spatial distribution with a progressive concentration of individuals in cells of highest carrying capacities. On the other hand, much more surprisingly, the increase in adult mortality had a heterogeneous impact at the cell level: the local population decrease varied spatially (Fig. 5c2-3) despite a spatially homogeneous increase in mortality, spatial heterogeneity increasing with the level of induced mortality (Fig. 5c2 vs. 5c3).

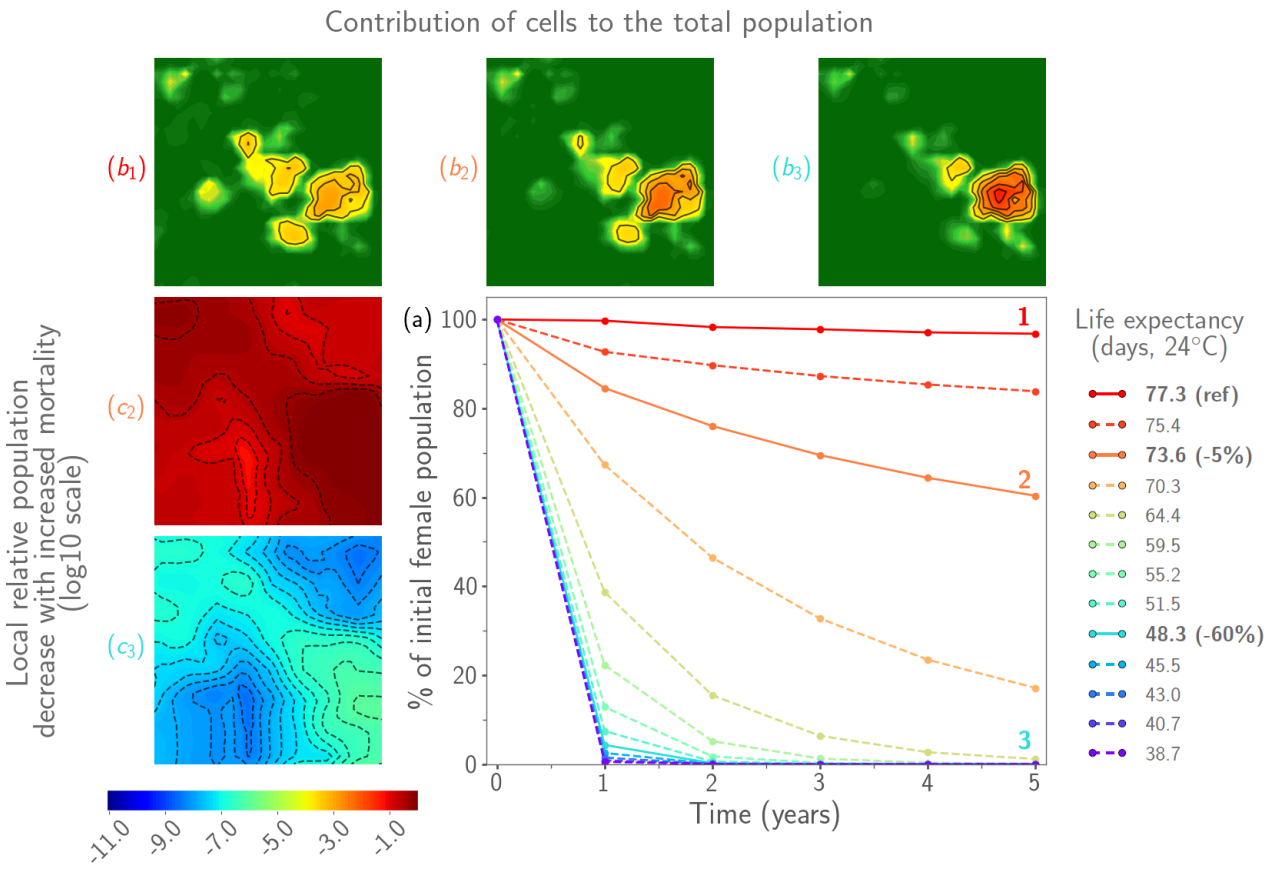

Figure 5. Impact of increasing adult mortality on population size in time and space. (a) relative decrease in female population size compared to the reference scenario while decreasing life expectancy at 24°C (corresponds to increases in adult mortality). Thick lines correspond to (1): no change, (2): +5% of adult mortality, (3): +60%. Spatial patterns during the last time step was assessed for these three scenarios (X from 1 to 3): (b_x) cells contributing the most to female population over the study area in scenario X ($\frac{(T_{t_{max},c}+F_{1:4+,t_{max},c})_{scenarioX}}{(\sum_c T_{t_{max},c}+F_{1:4+,t_{max},c})_{scenarioX}}$) are in red; ($c_x$) cells with the highest local impact of increased mortality in scenario x compared to the reference scenario ($\frac{(T_{t_{max},c}+F_{1:4+,t_{max},c})_{scenarioX}}{(T_{t_{max},c}+F_{1:4+,t_{max},c})_{reference}}$) are in blue (log10 scale).

To better understand this latter pattern, three local cell factors related to environmental heterogeneity were examined: carrying capacity, mean annual temperature, and standard deviation of annual temperature (Fig. 6). While the carrying capacity had no influence here (Fig. 6a), the local temperature largely contributed to explain the pattern (Fig. 6b-d). Both a decrease in the mean and standard deviation of the local annual temperature were associated with a decrease in the local impact of increasing adult mortality, despite the narrow ranges of variation in the mean (23.7°C to 24.3°C) and standard deviation (1.98°C to 2.37°C). There was no correlation between these two temperature statistics (Fig. 6c-d).

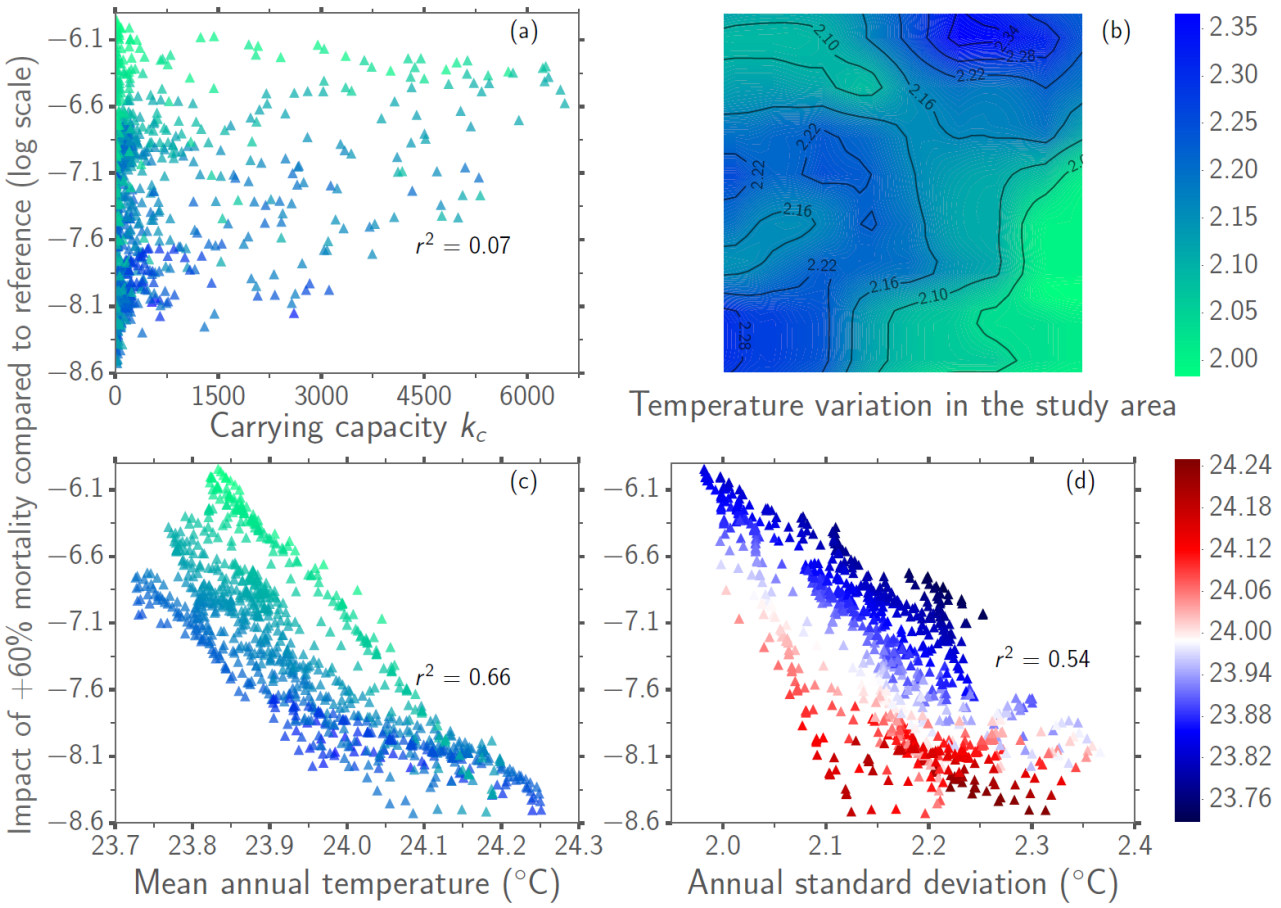

Figure 6. Correlation between environmental variables and the local impact of increasing mortality by 60% (measured as $\frac{(T_{t_{max},c}+F_{1:4+,t_{max},c})_{scenario3}}{(T_{t_{max},c}+F_{1:4+,t_{max},c})_{reference}}$): (a) local carrying capacity k_c; (b) spatial representation of the annual standard deviation of local temperatures; (c) annual mean temperature; (d) annual standard deviation of temperature. In (a, c, d), the local impact of mortality is on the y-axis (log10 scale), the higher being the value, the smaller the impact. Each point corresponds to a cell of the simulated grid, point colour denoting in (a-b) for the annual standard deviation of local temperature (same colour bar as in (b)), while in (d) to the mean annual temperature of cells (specific colour bar). Correlation coefficient r^2 between axes is shown for (a, c, d).

4. Discussion

Environmental heterogeneity with respect to carrying capacity and temperature not only drives the temporal population dynamics of *G. p. gambiensis* at large scale, but also the spatial distribution of individuals and unexpectedly renders heterogeneous the impact of a homogeneous increase in adult mortality. Such a heterogeneous impact can be compensated during eradication campaigns by homogeneous induced sterility when sterile males are released by air and aggregate in the same sites than wild males (Vreysen et al. 2011), thus warranting a homogeneous sterile to wild ratio, as was observed in the eradication campaign against *Glossina austeni* on Unguja Island of Zanzibar. We

300 argue that control strategies should account for environmental heterogeneity to increase the chances
301 of success, with emphasis on local areas of high suitability characterized by a high carrying capacity
302 and on local refuges characterized by a cold local temperature within the relevant range for tsetse
303 (23.7-24.0°C here) and a low local variability of temperature over the year (irrespective of carrying
304 capacity). Refuges, highlighted in our study area despite a small surface suitable for tsetse, could
305 jeopardize control efforts by providing areas from which recolonization may occur after control has
306 stopped.
307 In addition, temperature effect on population dynamics both at large and small local scales reinforces
308 the need for investigating further the impact climate change could have on tsetse populations
309 (Terblanche et al. 2008; Moore et al. 2012). It is unlikely that tsetse flies will cross the Sahara, but
310 they could migrate to higher altitudes and invade trypanosoma-free zones, particularly in Eastern and
311 Southern Africa where tsetse distribution is mainly governed by altitude (Solano et al. 2010a). Such
312 population shifts will impact the density of cattle in either direction, which may in turn impact the
313 distribution of wild fauna including lions (Carter et al. 2018). Populations previously isolated from
314 one another could also merge, making developed and adopted control strategies challenging, and
315 conversely, new isolated populations could appear, all the more as temperature is the first driver of
316 landscape friction in tsetse (Bouyer et al. 2015).
317 The mechanistic spatio-temporal model developed to predict *G. p. gambiensis* population dynamics
318 and how these evolve when adult mortality is increased is original compared to already published
319 models. First, it incorporated environmental heterogeneity through a data-driven approach, both
320 accounting for variable temperatures and carrying capacities in space and time. Using realistic
321 patterns instead of theoretical ones (Childs 2011), knowledge-driven ones (Barclay & Vreysen 2013),
322 or aggregated ones assuming a binary occupancy (Lin et al. 2015) evidenced unexpected refuges. The
323 proposed model can be applied to other areas with available data and a known metapopulation
324 structure. Second, new field and laboratory data on mortality, development, and dispersal have been
325 incorporated into the model. Predicted age structure was in very good agreement with field data, and

was robust in our simulations, barely impacted by parameter variations. Amplitude and duration of seasons are expected to be major drivers of parity distribution, which could not be assessed here as temperature data were available for only a year. Our results highlight the need for more biological studies to better infer mortality variations with temperature, as well as the crucial need for new methods to thoroughly estimate temperatures as perceived by individuals. Such a complementarity interplay between models, field observations, and laboratory experiments is fundamental to achieve trustworthy predictions.

The fact that mortality has a stronger influence on population dynamics than reproduction is consistent with tsetse flies being specialists with a narrow niche. They are willing to avoid mortality at all costs (Pagabeleguem et al. 2016), where other species compensate for losses by boosting birth rates (Southwood et al. 1974). *Glossina* spp. have evolved towards an optimal utilization of energy and resources (Cody 1966), which makes them highly adapted to their ecological niche. Therefore, they are less likely to leave their habitat and expose themselves to other environments, which keeps the population at or near carrying capacity (Southwood et al. 1974).

Efficient control methods can only be designed by considering a species ecological strategy (Southwood et al. 1974; Conway 1977). Fast action methods such as chemicals are better suited for species showing high reproductive rates, short generation times, along with broad food preferences and good dispersing abilities (Altieri et al. 1983). In contrast, pests reproducing at lower rates and having longer generation time but good competitive abilities would be more efficiently restrained with cultural control (e.g. insect pests), host resistance, and sterilization (Altieri et al. 1983). Nonetheless, such quite extreme characteristics should be considered in conjunction with species relationships within communities (Ehler & Miller 1978; Altieri et al. 1983).

Traps, targets, and insecticide-treated livestock are control tactics that increase adult mortality, which can drastically reduce tsetse populations (Kagbadouno et al. 2011; Dicko et al. 2014; Percoma et al. 2018). However, our results indicate also generation time as a contributing factor to population size variations. Such a factor can be indirectly modified using the sterile insect technique, which impair

352 reproduction (Dyck et al. 2005). Obtaining very low tsetse densities is not enough to reach eradication
353 as was demonstrated recently by the failures of three eradication programs against *G. p. gambiensis*
354 in north-western Ghana (Adam et al. 2013), Loos islands in Guinea (Kagbadouno et al. 2011), and
355 the Mouhoun river in Burkina Faso (Percoma et al. 2018). In addition, in view of unexpected local
356 refuges where increasing adult mortality is not as effective as in other areas, it becomes necessary to
357 further assess the effect of combined and spatially targeted control measures to achieve eradication.
358 Our model provides a relevant tool to evaluate such complex control strategies as it originally
359 accounts simultaneously for density-dependent processes, spatial and temporal environmental
360 heterogeneity, and all stages of tsetse lifecycle possibly targeted by control measures. Our framework
361 could also be useful to identify where to focus stakeholders' efforts to minimize impact of other
362 specialist pests, such as the codling moth (*Cydia pomonella*) affecting apple and pear trees, and the
363 sheep ked (*Melophagus ovinus*). Nevertheless, the importance of stochastic events when populations
364 become very small must not be overlooked and these effects should be included in future
365 developments. Our approach gives clues on how to trigger a drastic decline of the population.
366 However, to predict the subsequent population dynamics at low densities and assess final steps of
367 eradication strategies, a deterministic framework becomes irrelevant as it does not enable quantifying
368 the probability of population extinction at local and large scales.
369 Accounting for spatial heterogeneity is essential to better understand and predict tsetse population
370 dynamics, as habitat fragmentation holds the key to population survival when conditions are globally
371 hostile. However, parameters driving tsetse fly dispersal abilities did not structure their final
372 distribution. Landscape ecology must be studied to reveal preferential target zones and identify
373 patches that will need longitudinal surveillance. Optimal management strategies are therefore valid
374 for a given species in a given habitat and should not be generalized without baseline data collection
375 to characterize the ecosystem.
376 To conclude, environmental carrying capacity largely explains the contribution of local source spots
377 to tsetse population dynamics at a large scale, but unfavourable conditions progressively lead such

spots to disappear, refuges then being localized in zones with colder and less variable temperature where population decrease due to increasing adult mortality is reduced. Targeted areas for control should be chosen with caution when facing such a heterogeneous habitat.

Authors' contribution

JB and PE designed the study and advised biological details. HC, SA, SPi and PE developed the model. HC conducted the analyses and prepared the figures. HC, SA, SPi, JB and PE discussed the results. HC and PE wrote the manuscript. AD provided model external input data readily usable by the mechanistic model. JB, MTS, BS, MB, MV, SPa, AB collected the data. All authors edited the manuscript.

Acknowledgements

The authors are thankful to the technicians of the vet services from Senegal and ISRA for collecting the field data used in this study.

Funding

This work has been conducted within the project 'Integrated Vector Management: innovating to improve control and reduce environmental impacts' (IVEMA) of Carnot Institute 'Livestock Industry for the Future' (F2E). This project received funding from the European Research Council under the European Union's Horizon 2020 research and innovation programme (grant agreement No 682387—REVOLINC).

References

Adam, Y., Cecchi, G., Kgori, P. M., Marcotty, T., Mahama, C. I., Abavana, M. et al. (2013). The sequential aerosol technique: a major component in an integrated strategy of intervention against riverine tsetse in Ghana. PLoS Negl. Trop. Dis. 7: e2135.

400 Allsopp, R. (2001). Options for vector control against trypanosomiasis in Africa. Trends Parasitol.
401 17(1):15-9.
402 Alsan, M. (2015). The effect of the tsetse fly on African development. American Economic Review
403 105, 382-410.
404 Altieri, M. A., Martin, P. B., Lewis, W. J. (1983). A quest for ecologically based pest management
405 systems. Environmental management 7, 91–100.
406 Barclay, H., Hargrove, J. (2005). Probability models to facilitate a declaration of pest-free status, with
407 special reference to tsetse (Diptera: Glossinidae). Bulletin of Entomological Research 95, 1–11.
408 Barclay, H. J., Vreysen, M. J. B. (2013). The interaction of dispersal and control methods for the
409 riverine tsetse fly Glossina palpalis gambiensis (Diptera: Glossinidae): a modelling study. Popul.
410 Ecol. 55, 53-68.
411 Bouyer, J. (2006). Ecologie des glossines du Mouhoun au Burkina Faso : intérêt pour l'épidémiologie
412 et le contrôle des trypanosomes africaines. PhD thesis. Univ. Montpellier II, Sciences et
413 Techniques du Languedoc, France.
414 Bouyer, J., Bouyer, F., Donadeu, M., Rowan, T., Napier, G. (2013a). Community- and farmer-based
415 management of animal African trypanosomosis in cattle. Trends in Parasitology 29, 519-522.
416 Bouyer, J., Guerrini, L., César, J., de la Rocque, S., Cuisance, D. (2005). A phyto-sociological
417 analysis of the distribution of riverine tsetse flies in Burkina Faso. Medical and Veterinary
418 Entomology 19, 372-378.
419 Bouyer, J., Pruvot, M., Bengaly, Z., Guerin, P. M., Lancelot, R. (2007). Learning influences host
420 choice in tsetse. Biology Letters 3, 113-116.
421 Bouyer, J., Seck, M. T., Sall, B. (2013b). Misleading guidance for decision making on tsetse
422 eradication: Response to Shaw et al. (2013). Preventive Veterinary Medicine 112, 443– 446.
423 Bouyer, J., Seck, M. T., Sall, B., Guerrini, L., Vreysen, M. J. B. (2010). Stratified entomological
424 sampling in preparation of an area-wide integrated pest management programme: the example of

Glossina palpalis gambiensis in the Niayes of Senegal. Journal of Medical Entomology 47(4), 543-552.

Bouyer, J., Dicko, A. H., Cecchi, G., Ravel, S., Guerrini, L., Solano, P. et al. (2015). Mapping landscape friction to locate isolated tsetse populations candidate for elimination. Proc. Natl. Acad. Sci. U. S. A. 112: 14575-14580.

Budd, L. (1999). DFID-funded tsetse and trypanosome research and development since 1980. Volume 2: Economic Analysis, Livestock Production Programme. (NRInternational).

Cailly, P., Tran, A., Balenghien, T., L'Ambert, G., Toty, C., Ezanno, P. (2012). A climate driven abundance model to assess mosquito control strategies. Ecol. Model. 227, 7-17.

Carter, N. H., Bouley, P., Moore, S., Poulos, M., Bouyer, J., Pimm, S. (2018). Climate change, disease range shifts, and the future of the Africa lion. Cons. Biol. doi: 10.1111/cobi.13102.

Charron, M. V. P., Balenghien, T., Seegers, H., Langlais, M., Ezanno, P. (2013). How Much Can Diptera-Borne Viruses Persist over Unfavourable Seasons? PloS ONE 8(9):e74213. doi:10.1371/journal.pone.0074213

Childs, S. J. (2011). Theoretical levels of control as a function of mean temperature and spray efficacy in the aerial spraying of tsetse fly. Acta Tropica 117, 171–182.

Clark J.S. 2005. Why environmental scientists are becoming Bayesians. Ecology Letters 8, 2–14.

Cody, M. L. (1966). A general theory of clutch size. Evolution 20, 174–184.

Conway, G. R. (1977). Mathematical models in applied ecology. Nature 269, 291–297.

Crone, E. (2016). Contrasting effects of spatial heterogeneity and environmental stochasticity on population dynamics of a perennial wildflower. J. Ecol. 104, 281-91.

Dicko, A. H., Lancelot, R., Seck, M. T., Guerrini, L., Sall, B., Lo, M. et al. (2014). Using species distribution models to optimize vector control: the tsetse eradication campaign in Senegal. Proceedings of the National Academy of Sciences 111, 10149-10154.

449 Dicko, A. H., Percoma, L., Sow, A., Adam, Y., Mahama, C., Sidibé, I. et al.. (2015). A Spatio-
450 temporal Model of African Animal Trypanosomosis Risk. Plos Neglected Tropical diseases 9,
451 e0003921.
452 Dyck, V. A., Hendrichs, J., Robinson, A. S. (2005). Sterile insect technique. Springer, Dordrecht.
453 Ehler, L. E., Miller, J. C. (1978). Biological control in temporary agroecosystems. Entomophaga 23,
454 207–212.
455 Evans, M. R., Norris, K. J., Benton, T. G. (2012). Predictive ecology: systems approaches. Phil.
456 Trans. R. Soc. B 367, 163–169, doi:10.1098/rstb.2011.0191
457 Getz, W. M., Marshall, C. R., Carlson, C. J., Giuggioli, L., Ryan, S.J., Romanach, S.S. et al. (2018).
458 Making ecological models adequate. Ecol. Lett. 21, 153-66.
459 Glasgow, J. P. (1963). The distribution and abundance of tsetse. Pergamon Press, Oxford.
460 Griffith, A. B., Salguero-Gomez, R., Merow, C., McMahon, S. (2016). Demography beyond the
461 population. J. Ecol. 104, 271–280.
462 Guerrini, L., Bord, J. P., Ducheyne, E., Bouyer, J. (2008). Fragmentation analysis for prediction of
463 suitable habitat for vectors: example of riverine tsetse flies in Burkina Faso. J Med Entomol.
464 45(6):1180-6.
465 Hargrove, J. W. (1990). Age-dependent changes in the probabilities of survival and capture of the
466 tsetse, *Glossina morsitans morsitans* Westwood. Insect Science and Its Application 11, 323–330.
467 Hargrove, J. W. (2001). Factors affecting density-independent survival of an island population of
468 tsetse flies in Zimbabwe. Ent. Exp. & Appl. 100, 151–164.
469 Hargrove, J. W. (2003). Tsetse eradication: sufficiency, necessity and desirability. Centre for Tropical
470 Veterinary Medicine, Edinburgh.
471 Hargrove, J. W. (2004). Tsetse population dynamics. In: The Trypanosomiases. Ed. by I. Maudlin, P.
472 Holmes, and P. Miles. Oxford, UK: CABI Publishing, pp. 113–137.

473 Hargrove, J. W., Ackley, S. F. (2015). Mortality estimates from ovarian age distributions of the tsetse
474 fly *Glossina pallidipes* Austen sampled in Zimbabwe suggest the need for new analytical
475 approaches. Bulletin of Entomological Research 105, 294–304.
476 Hargrove, J. W., Coates, T. W. (1990). Metabolic rates of tsetse flies in the field as measures by the
477 excretion of injected caesium. Physiological Entomology 15, 157–166.
478 Harley, J. M. B. (1968). The influence of temperature on reproduction and development in four
479 species of Glossina (Diptera:Muscidae). Proc. R. Ent. Soc. Lond. (A) 43, 170–177.
480 Hartemink, N., Vanwambeke, S. O., Purse, B. V., Gilbert, M., Van Dyck, H. (2015). Towards a
481 resource-based habitat approach for spatial modelling of vector-borne disease risks. Biological
482 Reviews 90(4), 1151-62.
483 Hastings, A. (2012). Temporally varying resources amplify the importance of resource input in
484 ecological populations. Biol. Lett. 8, 1067–1069, doi:10.1098/rsbl.2012.0669
485 Hay, S. I., Tucker, C. J., Rogers, D. J., Packer, M. J. (1996). Remotely sensed surrogates of
486 meteorological data for the study of the distribution and abundance of arthropod vectors of disease.
487 Annals of Tropical Medicine & Parasitology 90, 1–19.
488 Hendrichs, J., Kenmore, P., Robinson, A. S., Vreysen, M. J. B. (2007). Area-wide integrated pest
489 management (AW-IPM): principles, practice and prospects, pp. 3-33. In M.J.B. Vreysen, A.S.
490 Robinson, and J. Hendrichs (eds.), Area-wide control of insect pests. From research to field
491 implementation. Springer, Dordrecht, The Netherlands.
492 Holt, R. D. (1985). Population dynamics in two-patch environments: some anomalous consequences
493 of an optimal habitat distribution. Theoretical Population Biology, 28, 181–208.
494 Kagbadouno, M. S., Camara, M., Bouyer, J., Courtin, F., Morifaso, O., Solano, P. (2011). Tsetse
495 control in Loos islands, Guinea. Parasites & Vectors 4, 18.
496 Keppel, G., Anderson, S., Williams, C., Kleindorfer, S., O'Connell, C. (2017). Microhabitats and
497 canopy cover moderate high summer temperatures in a fragmented Mediterranean landscape.
498 PLoS ONE 12(8):e0183106. doi:10.1371/journal.pone.0183106.

499 Kilibarda, M., Hengl, T., Heuvelink, G. B. M., Gräler, B., Pebesma, E., Perčec Tadić, M. et al. (2014).
500 Spatiotemporal interpolation of daily temperatures for global land areas at 1 km resolution. Journal
501 of Geophysical Research: Atmospheres 119, 2294–2313.
502 Klassen, W. (2005). Area-wide integrated pest management and the sterile insect technique, pp. 39-
503 68. In: V. A. Dyck, J. Hendrichs and A. S. Robinson (eds.), Sterile insect technique. Principles and
504 practice in area-wide integrated pest management. Springer, Dordrecht, The Netherlands.
505 Laveissière, C., Grébaut P. (1990). Recherches sur les pièges à glossines (Diptera, Glossinidae). Mise
506 au point d'un modèle économique : le piège "Vavoua". Trop. Med. Parasitol. 41: 185-192.
507 Lin, S., De Visser, M. H., Messina, J. P. (2015). An agent-based model to simulate tsetse fly
508 distribution and control techniques: A case study in Nguruman, Kenya. Ecological Modelling 314,
509 80–89.
510 Lloyd-Smith, J. O. (2010). Modeling density dependence in heterogeneous landscapes: Dispersal as
511 a case study. Journal of Theoretical Biology 265, 160–166.
512 Lord, J. S., Mthombothi, Z., Lagat, V. K., Atuhaire, F., Hargrove, J. W. (2017). Host-seeking
513 efficiency can explain population dynamics of the tsetse fly Glossina morsitans morsitans in
514 response to host density decline. PLoS Negl Trop Dis 11(7): e0005730.
515 Meyer, A., Holt, H. R., Oumarou, F., Chilongo, K., Gilbert, W., Fauron, A. et al. (2018). Integrated
516 cost-benefit analysis of tsetse control and herd productivity to inform control programs for animal
517 African trypanosomiasis. Parasites & Vectors 11:154. https://doi.org/10.1186/s13071-018-2679-x
518 Meyer, A., Holt, H. R., Selby, R., Guitian, J. (2016). Past and ongoing tsetse and animal
519 trypanosomiasis control operations in five African countries: a systematic review. PLoS Negl Trop
520 Dis 10(12):e0005247. doi:10.1371/journal.pntd.0005247
521 Moore, S., Shrestha, S., Tomlinson, K. W., Vuong, H. (2012). Predicting the effect of climate change
522 on African trypanosomiasis: integrating epidemiology with parasite and vector biology. J. Roy.
523 Soc. Interface 9, 817-830.

524 Pagabeleguem, S. (2012). Etude de compétitivité des mâles stériles dans le cadre de l'utilisation de
525 la technique de l'insecte stérile pour l'éradication des glossines dans la zone des Niayes au
526 Sénégal. Univ. Montpellier II, France – Univ. Abomey Calavi, Bénin. p. 31.
527 Pagabeleguem, S., Ravel, S., Dicko, A. H., Vreysen, M. J. B., Parker, A., Takac, P. et al. (2016).
528 Influence of temperature and relative humidity on survival and fecundity of three tsetse strains.
529 Parasites & Vectors 9, 520.
530 Pagabeleguem, S., Seck M. T., Sall B., Vreysen M. J. B., Gimonneau G., Fall A. G. et al. (2015).
531 Long distance transport of irradiated male Glossina palpalis gambiensis pupae and its impact on
532 sterile male yield Parasites & Vectors 8, 259.
533 Peck, S. L. (2012). Networks of habitat patches in tsetse fly control: implications of metapopulation
534 structure on assessing local extinction. Ecol. Model. 246, 99-102.
535 Peck, S. L., Bouyer, J. (2012). Mathematical modeling, spatial complexity, and critical decisions in
536 tsetse control. J. Econ. Entomol. 105, 1477-86.
537 Percoma, L., Sow, A., Pagabeleguem, S., Dicko, A. H., Serdébéogo, O., Ouédraogo, M. et al. (2018).
538 Impact of an integrated control campaign on tsetse populations in Burkina Faso. Parasites &
539 Vectors 11, 270.
540 Phelps, R. J., Burrows, P. M. (1969a). Prediction of the pupal duration of Glossina morsitans
541 orientalis Vanderplank under field conditions. J. Applied Ecol. 6, 323–337.
542 Phelps, R. J., Burrows, P. M. (1969b). Puparial duration in *Glossina morsitans orientalis* under
543 conditions of constant temperature. Ent. Exp. & Appl. 12, 33–43.
544 Phelps, R. J., Clarke, G. P. Y. (1974). Seasonal elimination of some size classes in males of *Glossina*
545 *morsitans morsitans* Westw. (Diptera, Glossinidae). Bulletin of Entomological Research 64, 313–
546 24.
547 Pulliam, H. R. (1988). Sources, sinks and population regulation. Am. Nat., 132, 652-661
548 Reichard, R. E. (2002). Area-wide biological control of disease vectors and agents affecting wildlife.
549 Rev. sci. tech. Off. int. Epiz. 21(1), 179-185.

Restif, A., Hayman, D. T. S., Pulliam, J. R. C., Plowright, R. K., George, D. B., Luis, A. D. et al. (2012). Model-guided fieldwork: practical guidelines for multidisciplinary research on wildlife ecological and epidemiological dynamics. Ecol. Lett. 1-12, doi: 10.1111/j.1461-0248.2012.01836.x

Rogers, D. J. (1988). A general model for African Trypanosomiasis. Parasitol. 10, 193-212.

Rogers, D. J. (1990). A general model for tsetse populations. Insect Sci. Applic. 11, 331-346.

Rogers, D. J., Randolph, S. J. (1984). A review of density-dependent processes in tsetse populations. Insect Science and Its Application 5, 397–402.

Rogers, D. J., Randolph, S. E. (1991). Mortality rate and population density of tsetse flies correlated with satellite imagery. Nature 351, 739-741.

Rogers, D. J., Hay, S. I., Packer, M. J. (1996). Predicting the distribution of tsetse flies in West Africa using temporal Fourier processed meteorological satellite data. Annals of Tropical Medicine & Parasitology 90, 225–241.

Saltelli, A., Chan, R., Scott, F. M. (2008). Sensitivity analysis. Wiley. 494 p. ISBN: 978-0-470-74382-9.

Saunders, D. S. (1962). Age determination for female tsetse flies and the age compositions of samples of *Glossina pallidipes* Aust., *G. palpalis fuscipes* Newst. and *G. brevipalpis* Newst. Bull. Entomol. Res. 53, 579-595.

Solano, P., Bouyer, J., Itard, J., Cuisance, D. (2010a). Cyclical vectors of trypanosomosis. In: Infectious and parasitic diseases of livestock. Eds P.-C. Lefèvre, J. Blancou, R. Chermette, G. Uilenberg, pp. 155-183. Éditions Lavoisier (Tec & Doc), Paris.

Solano, P., Kaba, D., Ravel, S., Dyer, N., Sall, B., Vreysen, M. J. B. et al. (2010b). Tsetse population genetics as a tool to choose between suppression and elimination: the case of the Niayes area in Senegal. Plos Tropical Neglected diseases 4, e692.

Southwood, T. R. E., May, R. M., Hassell, M. P., Conway, G. R. (1974). Ecological strategies and population parameters. The American Naturalist 108, 791–804.

576 Sutherland, W. J., Freckleton, R. P. (2012). Making predictive ecology more relevant to policy
577 makers and practitioners. Phil. Trans. R. Soc. B 367, 322–330, doi:10.1098/rstb.2011.0181
578 Sutherland, W. J., Freckleton, R. P., Godfray, H. C. J., Beissinger, S. R., Benton, T., Cameron, D. D.
579 et al. (2013). Identification of 100 fundamental ecological questions. Journal of Ecology, 101,58–
580 67.
581 Terblanche, J. S., Clusella-Trullas, S., Deere, J. A., Chown, S. L. (2008). Thermal tolerance in a
582 south-east African population of the tsetse fly *Glossina pallidipes* (Diptera, Glossinidae):
583 Implications for forecasting climate change impacts. Journal of Insect Physiology 54, 114–127.
584 Tilman, D., Kareiva, P. (1997). Spatial ecology: the role of space in population dynamics and
585 interspecific interactions. Princeton University Press, Princeton, New Jersey, USA.
586 Vale, G. A., Torr, S. J. (2005). User-friendly models of the costs and efficacy of tsetse control:
587 application to sterilizing and insecticidal techniques. Medical and Veterinary Entomology 19,
588 293–305.
589 Vinatier, F., Tixier, P., Duyck, P. F., Lescourret, F. (2011). Factors and mechanisms explaining spatial
590 heterogeneity: a review of methods for insect populations. Methods in Ecology and Evolution 2,
591 11–22.
592 Vreysen, M. J. B., Saleh, K. M., Lancelot, R., Bouyer, J. (2011). Factory tsetse flies must behave like
593 wild flies: a prerequisite for the sterile insect technique. PLoS Negl. Trop. Dis. 5(2): e907.
594 Vreysen, M. J. B., Seck, M. T., Sall, B., Bouyer, J. (2013). Tsetse flies: their biology and control
595 using area-wide integrated pest management approaches. Journal of Invertebrate Pathology 112, S15–
596 S25.